PROPULSION SYSTEM OPTIMIZATION FOR THE MUFLY MICRO HELICOPTER

D. Schafroth, C. Bermes, S. Bouabdallah, and R.Siegwart
Swiss Federal Institute of Technology Zürich (ETHZ)
Tannenstr. 3, 8092 Zürich
Switzerland

Overview

An appropriate design of the propulsion system for micro helicopters is an important task since most of the power on the helicopter is used for propulsion. While it is common to optimize the rotor aerodynamics, the drive train is mostly neglected. This is not sufficient for the rotor design, since it is not guaranteed that the electro motor can drive the rotor at its optimal point. Thus it is crucial to include the drive train in the simulation. This is done by using numerical Blade Element Momentum Theory (BEMT) for aerodynamic simulation which is extended by the drive train equation for truthful simulations. The new code is then used to investigate different rotor blade parameters on the drive train on the muFly helicopter. The results show that for the given drive train a thin blade with moderate camber, strong taper and twist performs best in turns of thrust to electrical power ratio.

1. INTRODUCTION

Micro helicopters are designated for applications such as surveillance and security, search and rescue or inspection and exploration. Existing examples are the muFR helicopter developed by Epson [1], the CoaX 2 developed at ETHZ [2] and the MICOR developed by the University of Maryland [3]. All those helicopters are limited in their autonomy time due to the low performance of the rotors in the low Reynolds number regime, where viscosity effects such as laminar separation bubbles [4] or early separation, strongly reduce the efficiency. In fact, the power required for the propulsion of a micro helicopter is more than 90% of the total power consumption. Therefore, proper design of the propulsion group is very important.

One goal of the European project muFly is to investigate and optimize the propulsion group of a micro helicopter to achieve longer flight duration [5]. In most literature, e.g. [6], [7], [8], only aerodynamics is considered for the investigation and optimization of the propulsion system. However, finding the aerodynamically optimal blade is not sufficient for optimal propulsion design. If the electric motor can not drive the blade at its optimal operation point, the blade optimization is pointless. It is therefore crucial to include the motor and gearing constraints in the process of propulsion optimization.

Another problem faced by rotor designers is the quantification of blade efficiency. In aerodynamics, the Figure of Merit (FM), which is the ratio between the mean ideal induced power and the total power, is often used to quantify the efficiency. Its use is problematic [9], since the induced power at constant thrust can be increased by a higher induced velocity. At the same time, the total power is increased, which is undesired since it lowers the thrust to power ratio. Strictly speaking, the FM is only a reasonable choice if the power loading is kept constant [10]. To fulfill this condition a priori is not possible. In principle, the rotor blade design seeks for maximal thrust using minimal electrical power for a long autonomy time. Hence, the thrust to electrical power is an appropriate efficiency measurement, which includes the constraints of the drive train. Of course, for an appropriate judgment of the performance of the rotor, the total thrust has to be considered and the desired specifications have to be fulfilled.

2. BLADE ELEMENT MOMENTUM THEORY

As a first step a simulation tool to predict the aerodynamics of the rotor is developed. This tool has to be accurate, fast and flexible to simulate as many different rotor setups as possible. The approach used is a variation of the classical numerical Blade Element Momentum Theory (BEMT). The classical BEMT uses certain assumptions to obtain a closed algebraic equation [10], for example that the $C_L - \alpha$ polar is a linear function. This is only partly true, especially in the low Reynolds number regime. Our approach avoids such simplifications by solving the 'exact' BEMT equations for every blade element.

The main problem of the unknown inflow angle ϕ is solved iteratively by combining the panel method code XFOIL [11] with momentum theory. The blade is split into elements, initial conditions (e.g inflow angle ϕ_{BET}) are chosen and the thrust values $\mathrm{d}T$ are calculated using the aerodynamic coefficients predicted by XFOIL (Blade Element Theory). Those thrust values are then taken to calculate the predicted inflow angle ϕ_{MOM} by the momentum theory

$$\phi_{\mathrm{MOM},i} = \tan^{-1}\left(\frac{v_{\mathrm{I},i}}{\Omega r_i}\right), \tag{1}$$

$$v_{\mathrm{I},i} = \sqrt{\frac{\mathrm{d}T_i}{2\rho\,\mathrm{d}A_i}}, \tag{2}$$

where $\mathrm{d}A_i$ is the infinitesimal rotor disc area, ρ the air density, $v_{\mathrm{I},i}$ the induced flow velocity, r the distance to the hub and Ω the rotor speed at the considered blade element i.
The difference between the two inflow angles $\Delta\phi = \phi_{\mathrm{BET}} - \phi_{\mathrm{MOM}}$ is minimized by adapting the inflow angle ϕ_{BET}. The procedure of the BEMT simulation is shown as an overview in FIG. 1.

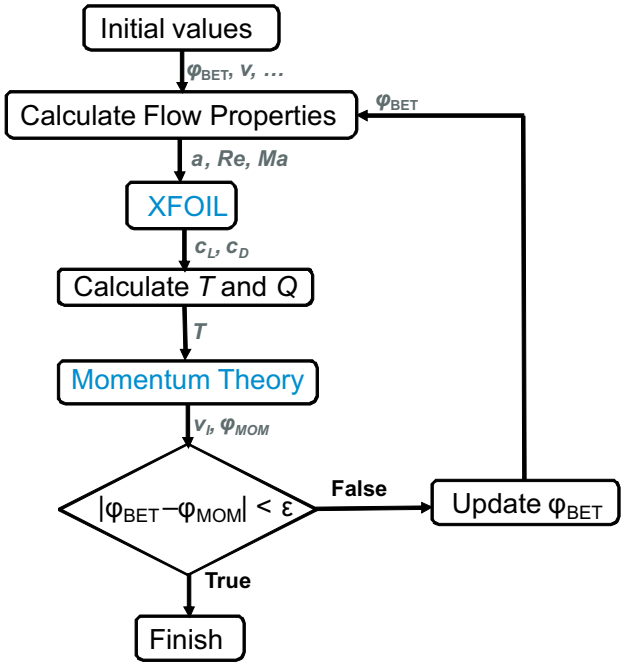

FIG. 1. Flowchart of the Blade Element Momentum Theory simulation.

Tip losses are taken into account using Prandtl's tip loss model [9]. The resulting code allows to simulate rotor configurations using different airfoil profiles and features like twist or taper without incorporating any experimental or other external data. Before the simulation can be used for the prediction of the rotor performance, the BEMT code has to be verified. Since there is only rare literature with experimental data available [12], a rotor test bench is built to measure thrust and drag torque of different rotor blade designs (Fig. 2).

The test bench is equipped with a force and a torque load cell sensor to measure the resulting thrust and drag torque of the tested rotors. Two motor controllers are used to run the rotors at the desired angular velocity, while the sensor data is collected by a data acquisition module. By measuring the current used for the motors, the drag torque of the single rotors can be determined even in coaxial mode. The rotor heads on the test bench are designed such that the blades can be mounted rapidly and precisely at different pitch angles. A rapid prototyping machine allows a fast manufacturing and provides the flexibility to generate complex shaped blades. The whole test bench is controlled by a PC allowing to run different measurement modes. Operation of the test bench in single rotor operation is also possible.
With the help of this test bench, the BEMT results are validated. In Fig. 3 the BEMT results for a single rotor with different rotor profiles are compared to the measured data showing the flexibility and accuracy of the BEMT code for all the profiles examined.

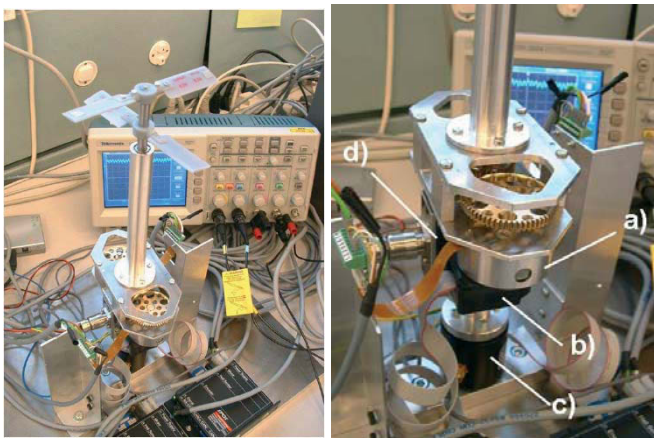

FIG. 2. Test bench for rotor blade optimization. (a) 2x Maxon EC 45 flat 30 W motor, (b) 2x optical encoders, (c) RTS 5/10 torque sensor, (d) FGP FN 3148 force sensor. The rotor blades are manufactured with a rapid prototype machine. Not shown data acquisition module NI USB 6009 and the two Maxon Epos 24/5 motor controllers.

Despite the good performance of the code, there exist also limitations: for instance, only moderate pitch angles can be simulated. As soon as the flow detaches from the airfoil, XFOIL is not able to predict the correct performance anymore. Additionally special features such as 'Gurney flaps' or special tip shapes can not be simulated.

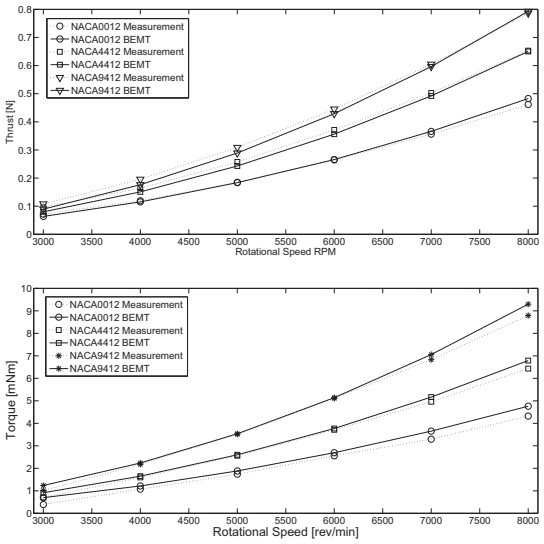

FIG. 3. Comparison of the BEMT results and the measurements for different blade profiles ($R = 0.06$m, $c = 0.02$m, $\theta = 14°$).

3. DRIVE TRAIN EXTENSION

After validation, the given electro motor and gears are integrated in the BEMT code. The differential equations for an electro motor [13] can be simplified and written as

$$J_{\mathrm{mot}}\dot{\omega} = \frac{\kappa_{\mathrm{M}}U - \kappa_{\mathrm{M}}\kappa_{\mathrm{E}}\omega}{R_{\Omega}} - d_R\omega - M_{\mathrm{L}}, \tag{3}$$

with the moment of inertia J_{mot}, electrical and mechanical motor constants κ_{E} and κ_{M}, the input voltage U, the electrical resistance R_{Ω}, the friction coefficient d_R and the external torque M_{L}.
For the extended BEMT simulation, only the stationary solution $\dot{\omega} = 0$ of (3) is of interest. The applying external torque M_{L} is the drag torque Q, caused by the rotor, reduced by the gear

$$M_L = \frac{Q}{\eta_{gear} i_{gear}}, \tag{4}$$

with the gear ratio i_{gear} and the gear efficiency η_{gear}. The drag torque of the rotor can be defined as [10]

$$Q = c_Q \pi \rho R^5 \Omega^2 = c_Q k_Q \Omega^2, \tag{5}$$

with the rotor radius R, the torque coefficient c_Q and the rotor speed Ω. Using the relation of the motor speed to the rotor speed $\omega = i_{gear}\Omega$, the resulting equation for the rotor speed Ω is

$$\frac{c_Q k_Q}{i_{\mathrm{gear}}\eta_{\mathrm{gear}}}\Omega^2 + \left(d_R i_{gear} - \frac{\kappa_{\mathrm{M}}\kappa_{\mathrm{E}} i_{\mathrm{gear}}}{R_{\Omega}}\right)\Omega - \frac{\kappa_{\mathrm{M}}U}{R_{\Omega}} = 0 \tag{6}$$

with the only unknown parameter c_Q, the torque coefficient. Measurements have shown that the rotor torque coefficient stays about the same over the considered range of rotational speeds, whereas the influence on the thrust coefficients is much stronger. The idea now is as follows: the rotor is defined and simulated by the BEMT simulation for a chosen rotational speed. The calculated torque coefficient is then used to calculate the resulting rotor speed on the drive train using Equation (6). This rotor speed is the new input for the BEMT simulation to calculate the final thrust. Now the thrust to electrical power ratio can be determined and the performance of the blade evaluated.

4. SIMULATIONS

The new code is used to investigate different rotor setups. There exist infinite possibilities for the rotor blade design. Especially the diversity of the blade profile makes the investigation difficult. In order to have a structure for the airfoil features such as maximum camber, thickness or camber maximum position the NACA four digit series [14] is used. The NACA four digit series describes the maximum camber (first digit), the camber position (second digit) and the maximal thickness of the profile (last two digits) in percentage of the chord length c.

Further investigated parameters are the rotor radius R and the chord length c. The latter can also be varied over the rotor blade length, known as taper. This can be done in various ways, but in this work only linear taper is considered, meaning that the chord length changes linearly with the radius R. The same can be done with the pitch angle of the blade resulting in a linear blade twist, another investigated parameter. There exist other possibilities to change the performance of the rotor blade such as lift-enhancing devices (Gurney Flaps, Turbulators or Winglets) or different tip shapes. Those possibilities can not be simulated with the BEMT code and are future work using Computational Fluid Dynamics (CFD).

5. RESULTS

In this chapter the simulation results for the tested rotor setups on the given drive train of the muFly helicopter are shown. In Fig. 4, the thrust to electrical power ratio and the thrust values for rotors with different radii at different pitch angles are plotted. In this case the bigger radii have their thrust to power optimum at lower pitch angles, whereas the smaller radii have it at high pitch angles. This reflects the influence of the drive train: the smaller blades produce less drag torque allowing the motor to run at higher speed at high pitch angles, where the bigger blades start to overload the motor. As expected, the thrust increases with increased radius. Depending on the desired thrust value a different radius is the most efficient choice. For example, if a thrust value of $T \approx 0.3$N is needed, a radius of $R = 0.06$m is the most efficient choice, while a much higher thrust can not be achieved in this configuration and a bigger radius has to be chosen. This applies for all the considered cases, making the thrust values an important criterion that needs to be included in the investigations.

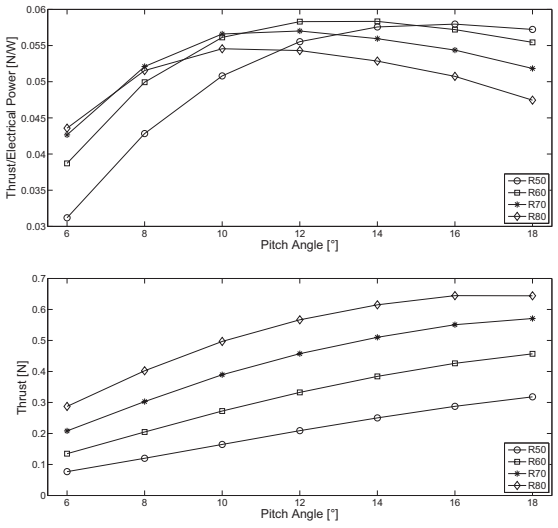

FIG. 4. Simulation results for a rotor (NACA0012, $c = 0.02$m) with different radii (R=0.05m,0.06m,0.07m,0.08m). Top: Thrust to electrical power ratio. Bottom: Thrust value

The result for the profile thickness (Fig. 5) shows the same outcome as claimed in [8]. In general, a thinner airfoil seems

to have a better performance than a thicker blade and is a result of the strong viscosity effects. In this configuration, the most efficient profile is the one with a thickness of 6% of the chord length. The thrust values are all in the same range.

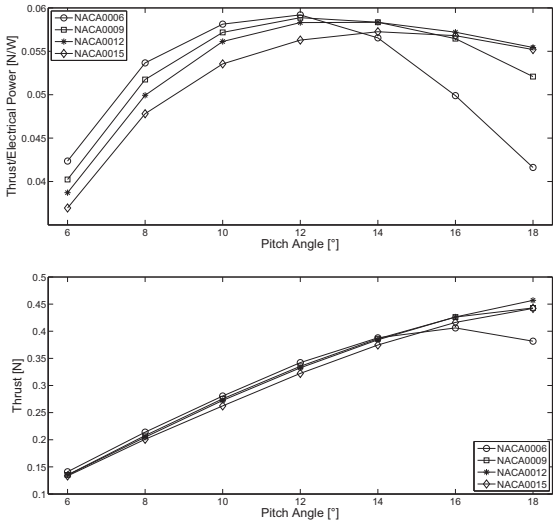

FIG. 5. Simulation results for a rotor with different radii thicknesses. Top: Thrust to electrical power ratio. Bottom: Thrust value.

The plot showing the maximum camber (Fig. 6) is more surprising. In [8] and [15], an arc profile with 10% (of the chord length) camber has been found much more efficient than a symmetrical uncambered profile. Considering the whole drivetrain the profile with 9% camber NACA9412 shows a worse performance than the symmetrical NACA0012 in a wide range of pitch angles. This is again the effect of the drive train, where the strong cambered blade overloads the electrical motor. A good choice is the NACA4412 that shows good performance in efficiency and thrust.

The influence of the maximum camber position on profiles with moderate camber of 4% as plotted in Figure 7 is weak. The NACA4412 with the maximum camber at $0.4c$ shows a similar performance as the NACA4912 with maximum camber at $0.9c$. Maybe the influence is stronger for more cambered profiles, but as seen before the stronger cambered profile showed a bad performance.

In Figure 8 the chord length of the rotor is varied. This is identical to changing the aspect ratio AR. Since the rotor radius is $R = 0.06$ the aspect ratio varies from 2.4 to 6. The results show that the chord length $c = 0.015$m ($AR = 4$) has the best performance over almost the whole pitch angle range.

The last two investigated parameters are blade twist and taper. In Fig. 9 the performance of blades with different tapers are plotted and compared to a blade with constant chord length. The labeling $TAPER2515$ stands for a blade with a chord length $c_{\mathrm{hub}} = 0.025$m at the hub and $c_{\mathrm{tip}} = 0.015$m at the rotor tip. The stronger the taper, the more efficient is the blade. On the downside the thrust gets lower due to the reduced chord. The reason for those two effects is the lower thrust at the fast moving tip and thus reduced tip losses (more efficient).

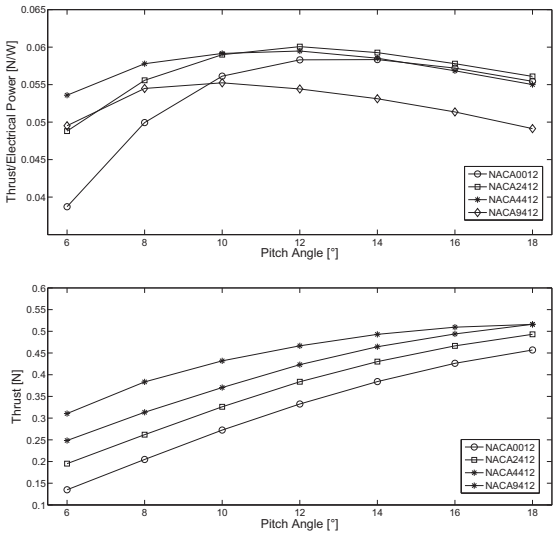

FIG. 6. Simulation results for a rotor with different maximal cambers. Top: Thrust to electrical power ratio. Bottom: Thrust value.

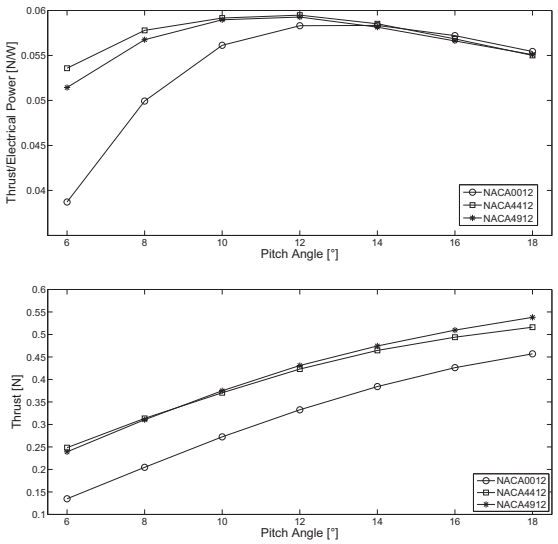

FIG. 7. Simulation results for a rotor with different maximal camber positions. Top: Thrust to electrical power ratio. Bottom: Thrust value.

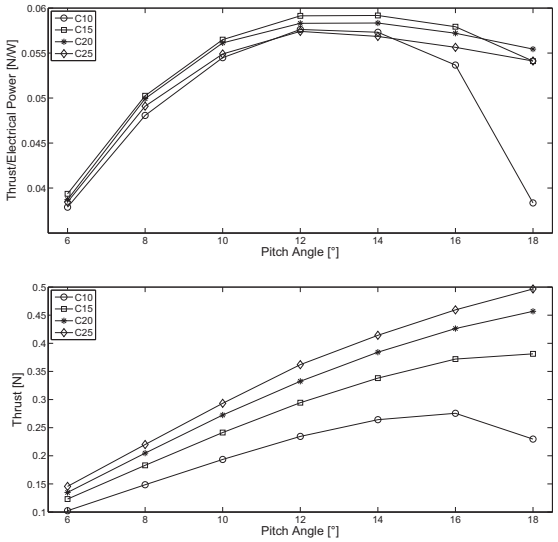

FIG. 8. Simulation results for an untwisted rotor with constant radius (R = 0.08m) and chord length (c = 0.02m) using different NACA profiles [14]. Top: Thrust to electrical power ratio. Bottom: Thrust value.

A strong influence on the performance is found by using twisted blades. Here the blade with 10° twist (higher pitch at the hub) outperformances the other two blades in the low pitch angles but suffers from the high drag in the high pitch angles.

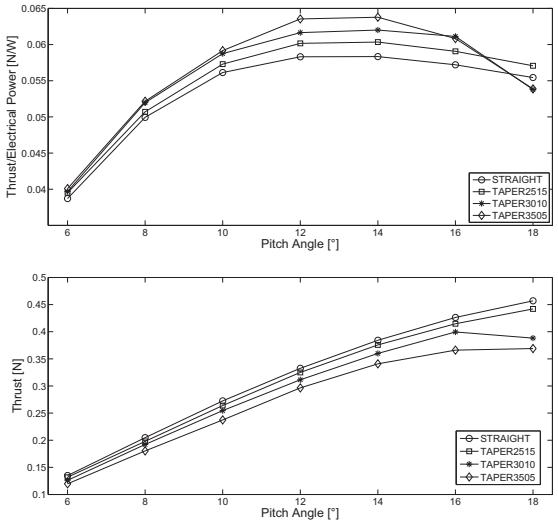

FIG. 9. Simulation results for rotors with different taper (NACA0012, $R = 0.02m$).Top: Thrust to electrical power ratio. Bottom: Thrust value.

In a last step, good design features of the tested parameters are combined to six new blades and plotted in Figure 11. The corresponding blade parameters are shown in Table 1.

The combination reflect the behavior found in the previous simulations. The thinnest blade $N°6$ with the strongest taper and twist performs the best over a wide range of pitch angles. Additionally, it produces the highest thrust. Otherwise, the already seen effects apply, such as a strong lift producing blade has the efficiency optimum at low pitch angles, where as the others have it at high pitch angle.

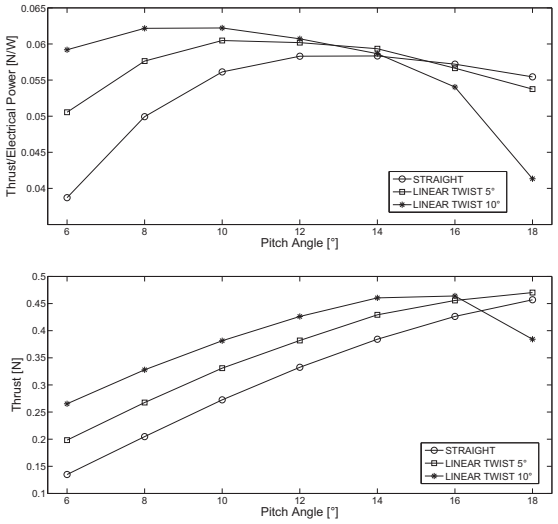

FIG. 10. Simulation results for rotors with different taper (NACA0012, $R = 0.02m$). Top: Thrust to electrical power ratio. Bottom: Thrust value.

N°	Airfoil	Taper	Twist
1	NACA4412	1510	10°
2	NACA4412	1510	5°
3	NACA4412	2010	10°
4	NACA4409	1510	10°
5	NACA4409	1510	5°
6	NACA4409	2010	10°

TAB. 1. Blade parameters for the tested blades in Fig. 11.

6. SUMMARY AND CONCLUSION

In this paper an approach for propulsion system design and optimization for a micro helicopter is presented. Instead of only considering the rotor aerodynamics as it is found in most literature, the whole drive train is included in the simulation. This approach allows to simulate the real condition on the helicopter and to calculate the wanted efficiency quantity the thrust to electrical power ratio. The simulation starts with a variation of the numerical Blade Element Momentum Theory (BEMT) in order to calculate the aerodynamic performance of the rotor. The resulting aerodynamic torque coefficient is then combined with the equation for the drive train to calculate the true rotor speed. With the help of this rotor speed, the true thrust is calculated.

In a next step, the influence of different rotor parameters on the performance of a rotor mounted on the drive train of the muFly helicopter is tested. The results show the strong influence of the drive train and that the presented method is more suitable for the rotor design for micro helicopter than common approaches only considering the aerodynamics. If the drive train is not fix on the helicopter it is recommendable to include

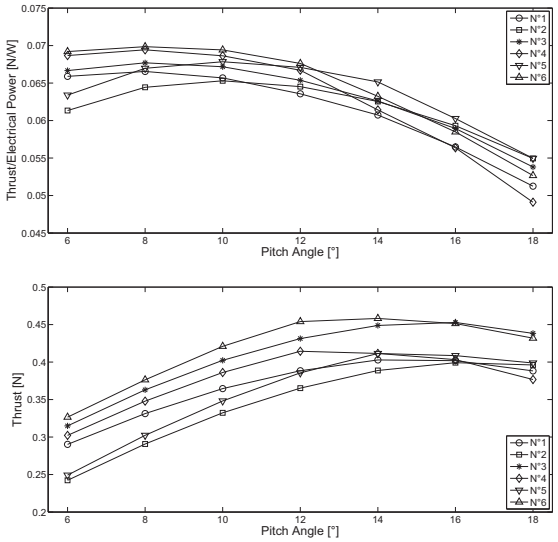

FIG. 11. Simulation results different rotor parameter combination (legend in Tab. 1). Top: Thrust to electrical power ratio. Bottom: Thrust value.

a variation of the gearing in the simulation and design of the propulsion system.
Future work is to simulate blades with complex shapes such as Winglets, Gurney Flaps, different tip shapes and coaxial configuration with the help of CFD simulations.

7. REFERENCES

[1] Epson. http://www.epson.co.jp/e/newsroom/news_2004_08_18.htm, (01/28/2009), 2004.

[2] C. Bermes, S. Leutenegger, S. Bouabdallah, D. Schafroth, and R. Siegwart, "New Design of the Steering Mechanism for a Mini Coaxial Helicopter," in *IEEE International Conference on Intelligent Robots and Systems (IROS)*, Nice, France, 2008.

[3] F. Bohorquez, P. Samuel, and J. Sirohi, "Design, Analysis and Performance of a Rotary Wing MAV," *Journal of the American Helicopter Society*, vol. 48, 2003.

[4] W. Shyy, Y. Lian, J. Tang, D. Viiieru, and H. Liu, *Aerodynamics of Low Reynolds Number Flyers*. Cambridge: Cambridge University Press, 2008, vol. Vol. 1.

[5] D. Schafroth, S. Bouabdallah, C. Bermes, and R. Siegwart, "From the Test Benches to the First Prototype of the muFly Micro Helicopter," *Journal of Intelligent and Robotic Systems*, vol. 54, no. 1-3, pp. 245–260, 2008.

[6] P. Pounds, R. Mahony, and J. Gresham, "Towards Dynamically-Favourable Quad-Rotor Aerial Robots," in *Australasian Conference on Robotics and Automation*, D. A. Nick Barnes, Ed., Canberra, Australia, 2004.

[7] F. Bohorquez, F. Rankinsy, J. Baederz, and D. Pines, "Hover Performance of Rotor Blades at Low Reynolds Numbers for Rotary Wing Micro Air Vehicles. An Experimental and CFD Study," 2003.

[8] N. Tsuzuki, S. Sato, and T. Abe, "Design Guidelines of Rotary Wings in Hover for Insect-Scale Micro Air Vehicle Applications," *Journal of Aircraft*, vol. 44, pp. 252–263, 2007.

[9] A. Bramwell, *Helicopter Dynamics*, 2nd ed. Butterworth Heinemann, 2001.

[10] J. Leishman, *Helicopter Aerodynamics*, 2nd ed. Cambridge, 2006.

[11] XFOIL. http://raphael.mit.edu/xfoil, (01/28/2009).

[12] C. P. Coleman, "A Survey of Theoretical and Experimental Coaxial Rotor Aerodynamic Research," Tech. Rep., 1997.

[13] G. Mueller and B. Ponick, *Elektrische Maschinen Grundlagen elektrischer Maschinen*. Weinheim: VCH, 2006.

[14] E. Jacobs, K. Ward, and R. Pinkerton, "The Characteristics of 78 Related Airfoil Sections from Tests in the Variable-Density Wind Tunnel," NASA, Tech. Rep., 1933.

[15] F. Bohorquez and D. Pines, "Hover Performance and Swashplate Design of a Coaxial Rotary Wing Micro Air Vehicle," 2004.